

Superradiance and Lasing in Driven-Dissipative Dicke models

Author: David Pérez Castro

Facultat de Física, Universitat de Barcelona, Diagonal 645, 08028 Barcelona, Spain.

Advisor: Maria Moreno-Cardoner

Abstract: We study the differences between the normal, the superradiant, and the lasing phases emerging in a model describing an ensemble of atoms interacting with a single quantized mode of light. The model interpolates between the two well known Dicke and Tavis-Cummings Hamiltonians. We obtain the phase diagram using a mean-field stability analysis and an exact numerical calculation, that allows us to evaluate observables such as the expected value of the number of photons and population inversion. We finish our work by analyzing and comparing the spectra of light emitted in each of these phases.

I. INTRODUCTION

The concept of superradiance is first introduced by Dicke in 1954 [1], when he described the problem of a gas of molecules interacting with a common radiation field. In contrast to previous studies, molecules are not treated as independent. The radiative properties (spontaneous emission rate) are strongly modified due to the presence of the common bath when atoms are confined in a small volume (compared to the light wavelength). This allows the existence of superradiant states with coherent spontaneous emission, that is, an emission rate that scales as the square of the molecule concentration, in stark contrast to independent atoms whose emission scales linearly.

What we now know as the Dicke model, refers to an ensemble of atoms paired to a single quantized light mode, such as the optical mode of a cavity [2]. It predicts a continuous phase transition between a normal and a superradiant state characterized by photon occupation of the cavity mode. This model also belongs to the same universality class as the Ising model.

Despite being closely related, lasing is not exactly equivalent to superradiance. A canonical model for lasing is the Tavis-Cummings Hamiltonian, analogous to the Dicke model without counter-rotating terms (those that do not conserve the total number of excitations), in presence of an additional incoherent pump. In standard lasing, besides photon occupation of the cavity mode, there exists atomic population inversion (that is, the probability of finding the atom in the excited state is higher than in the ground state). Furthermore, the light escaping the cavity shows different spectral properties in the two phases.

In this work we will revisit these two models and analytically derive the superradiant and lasing transition critical points using a mean-field approximation (sections II A and II B). We will then introduce a generalized model describing N atoms coupled to a cavity mode that exhibit both the superradiant and the lasing transition (section II C). The model interpolates between the Dicke and the Tavis-Cummings Hamiltonian, in presence of incoherent pump and where cavity losses and spontaneous

emission of the atoms into other modes apart from the cavity are also taken into account. Finally, we will construct a phase diagram and explore more deeply the characteristics of each of the phases, using different methods such as linear stability analysis and exact diagonalization (section III).

II. MODELS

A. Dicke Model and Superradiant Transition

The Dicke model [1, 2], which describes a collection of N two-level quantum emitters (usually atoms) interacting with a single bosonic mode (usually the cavity optical mode), can be written as (from now on, $\hbar = 1$):

$$H_D = \omega_c a^\dagger a + \frac{\omega_0}{2} \sum_{i=1}^N \sigma_i^z + \frac{\lambda}{\sqrt{N}} \sum_{i=1}^N (a + a^\dagger) \sigma_i^x. \quad (1)$$

Here a^\dagger (a) creates (destroys) a photon in the cavity mode and satisfies $[a, a^\dagger] = 1$. The atomic operators σ_i^z and σ_i^x are the usual Pauli matrices acting on atom i , and are given by $\sigma_i^x = \sigma_i^+ + \sigma_i^-$ and $\sigma_i^z = \sigma_i^+ \sigma_i^- - \sigma_i^- \sigma_i^+$, where σ_i^\pm are σ_i^\mp the corresponding creation and annihilation operators of an excitation of atom i , respectively. By transforming $a \rightarrow -a$ and $\sigma^x \rightarrow -\sigma^x$ we can see that the Hamiltonian remains invariant, and thus exhibits a discrete \mathbb{Z}_2 symmetry, related to the parity of the number of excitations.

Let us analyse each of the terms of the Hamiltonian in Eq.(1). The first term corresponds to the energy of the photons in the mode of the cavity, while the second term is associated with the internal energy of the atoms, counting the difference between atoms on the excited state and atoms on the ground state. The last term refers to the photon-atom interaction, and includes both co-rotating and counter-rotating interactions with the same coupling strength λ . The former are the more conventional energy-conserving terms, which describe the excitation of an atom by absorbing a cavity photon, and the desexcitation of the atom by emitting a photon in the cavity. Instead, the latter do not conserve energy,

and correspond to excitation of an atom with the gain of a cavity photon, and desexcitation of an atom with the loss of a cavity photon. Note that the coupling constant is rescaled by the factor $1/\sqrt{N}$. This is introduced in order to have a finite value of the critical coupling in the thermodynamic limit.

With our model defined, we will now find when the phase transition takes place in a mean-field approximation by minimizing the free energy with respect of α . This mean-field approximation is achieved by supposing that all the photons of the cavity are in a coherent state, which implies: $a|\alpha\rangle = a^\dagger|\alpha\rangle = \alpha|\alpha\rangle$, with α a real number and $|\alpha\rangle = e^{-\frac{|\alpha|^2}{2}} \sum_{n=0}^{\infty} \frac{\alpha^n}{\sqrt{n!}} |n\rangle$ a coherent light state. This assumption allows us to replace a and a^\dagger operators by the real number α in Eq. (1) and the Hamiltonian becomes:

$$H_D^{\text{MF}} = \omega_c \alpha^2 + \frac{\omega_0}{2} \sum_{i=1}^N \sigma_i^z + 2\alpha \frac{\lambda}{\sqrt{N}} \sum_{i=1}^N \sigma_i^x \equiv \omega_c \alpha^2 + \sum_{i=1}^N h_i \quad (2)$$

Where we have separated the photonic constant part and the atom-dependent part. We can now compute our partition function as $\mathcal{Z}(\alpha) = \text{Tr}(e^{-\beta H_D^{\text{MF}}})$, with $\beta = 1/K_B T$. With the mean field approximation, this result is greatly simplified, as we only need to diagonalize the 2x2 matrix:

$$\mathcal{Z}(\alpha) = e^{-\beta \omega_c \alpha^2} \text{Tr} \left[\exp \begin{pmatrix} -\beta \frac{\omega_0}{2} & -\beta 2 \frac{\lambda \alpha}{\sqrt{N}} \\ -2\beta \frac{\lambda \alpha}{\sqrt{N}} & \beta \frac{\omega_0}{2} \end{pmatrix} \right]^N. \quad (3)$$

By doing this we obtain the expression for the partition function:

$$\mathcal{Z}(\alpha) = e^{-\beta \omega_c \alpha^2} 2 \cosh(-\beta E_0)^N, \quad (4)$$

where $E_0 = \sqrt{\frac{\omega_0^2}{4} + 4 \frac{\lambda^2 \alpha^2}{N}}$. From this expression it is straightforward to obtain the free energy:

$$F(\alpha) = -\frac{1}{\beta} \ln \mathcal{Z}(\alpha) = \omega_c \alpha^2 - \frac{N}{\beta} \ln 2 \cosh(\beta E_0). \quad (5)$$

Applying the minimum condition with respect to α , we obtain the phase transition condition:

$$\frac{\partial F}{\partial \alpha} = 2\alpha \left(\omega_c - \frac{2\lambda^2}{E_0} \tanh(\beta E_0) \right) = 0. \quad (6)$$

This equation has two solutions. The first one, where $\alpha = 0$, means that we have a phase with no photons in the cavity, the *normal* phase. The study of this phase is of no interest for us because nothing is happening in the cavity. On the other hand, when $\alpha \neq 0$, we have a breaking in the aforementioned \mathbb{Z}_2 symmetry, leading to a continuous phase transition. This new *superradiant* phase, is characterized by an increase of photon emission by the system. In the thermodynamic limit ($N \rightarrow \infty$), and low temperature regime ($\beta \rightarrow \infty$) it is possible to evaluate the coupling constant λ_c from Eq.(6):

$$\lambda_c = \frac{1}{2} \sqrt{\omega_c \omega_0}. \quad (7)$$

As we will see later, the superradiant transition persists in presence of cavity losses and single atom radiative decay, with a renormalized value of the critical coupling λ_c .

We could think that having a phase where our light emission is enhanced would be useful for building lasers, but there are two very important drawbacks for it to be possible. The first one, is that this increase in emission is not bound to a particular wavelength, making it a bad choice for a laser. The other one, is that if we calculate $\langle \sigma^z \rangle$ we see that it is less than 0, meaning that in order to be stable there have to be less excited atoms than ground-state atoms, contrary to what we would expect from a laser atom population.

B. Tavis-Cummings Hamiltonian and Lasing

Another historically relevant model is the so called Tavis-Cummings, which can be defined by neglecting Dicke's counter-rotating terms, with only terms that conserve the total excitation number:

$$H_{\text{TC}} = \omega_c a^\dagger a + \frac{\omega_0}{2} \sum_{i=1}^N \sigma_i^z + \frac{\lambda}{\sqrt{N}} \sum_{i=1}^N (a \sigma_i^+ + a^\dagger \sigma_i^-). \quad (8)$$

Now, instead of a \mathbb{Z}_2 symmetry, we have a $U(1)$ symmetry, since a unitary transformation $a \rightarrow e^{i\theta} a$ and $\sigma^- \rightarrow e^{i\theta} \sigma^-$ would leave our Hamiltonian unchanged. Taking a similar approach as in the Dicke model, we will impose mean-field interaction for the light with the corresponding Hamiltonian:

$$H_{\text{TC}}^{\text{MF}} = \omega_c \alpha^2 + \frac{\omega_0}{2} \sum_{i=1}^N \sigma_i^z + \alpha \frac{\lambda}{\sqrt{N}} \sum_{i=1}^N \sigma_i^x. \quad (9)$$

We find a very similar partition function:

$$\mathcal{Z}(\alpha) = e^{-\beta \omega_c \alpha^2} 2 \cosh(-\beta \tilde{E}_0)^N, \quad (10)$$

now with $\tilde{E}_0 = \sqrt{\frac{\omega_0^2}{4} + \frac{\lambda^2 \alpha^2}{N}}$. Similarly as before, we find in the thermodynamic and zero temperature limits the critical value for the coupling constant to be:

$$\lambda_c = \sqrt{\omega_c \omega_0}, \quad (11)$$

which is the same as Eq. (7) except for a factor of $\frac{1}{2}$. This difference stems from the fact that there are now only two interacting terms in the Hamiltonian instead of four terms.

Importantly, this superradiant transition disappears in presence of spontaneous emission of photons into free space. In this case, the system trivially relaxes into the normal state, with all atoms in the ground state and no photons in the cavity. However, this model undergoes a *lasing* phase transition when adding an external incoherent pump to the atoms, leading to atomic population inversion ($\langle \sigma_i^z \rangle > 0$) and emission of light highly peaked at a particular frequency, two features that characterize a standard laser.

C. Generalized driven-dissipative Dicke model

We will now consider a more general Hamiltonian that smoothly interpolates between the two previously discussed models, by adding a relative strength between counter- and co-rotating terms λ'/λ that can be varied at will:

$$H_G = \omega_c a^\dagger a + \frac{\omega_0}{2} \sum_{i=1}^N \sigma_i^z + \frac{\lambda}{\sqrt{N}} \sum_{i=1}^N (a \sigma_i^+ + a^\dagger \sigma_i^-) + \frac{\lambda'}{\sqrt{N}} \sum_{i=1}^N (a^\dagger \sigma_i^+ + a \sigma_i^-). \quad (12)$$

We can easily see that the case $\lambda' = \lambda$ corresponds to the Dicke model, while with $\lambda' = 0$ we recover the Tavis-Cummings model. We will also make our system more realistic by including photon cavity losses (that is, a photon has certain probability to be transmitted through the mirrors of the cavity) and spontaneous emission of photons into other modes rather than the cavity one, at rates κ and Γ_\downarrow , respectively. Like discussed before, incoherent pumping of the atoms also needs to be added in order to avoid a trivial decay to the normal state whenever $\Gamma_\downarrow, \kappa \neq 0$ and also to ensure that we will have a lasing phase by enabling atomic population inversion. All these processes can be modeled in the Markov approximation using the so-called Lindblad super-operator, which in general acts on the density matrix as:

$$\mathcal{L}_{\hat{x}}[\rho] = \Gamma_x \left[\hat{x} \rho \hat{x}^\dagger - \frac{1}{2} \{ \hat{x}^\dagger \hat{x}, \rho \} \right], \quad (13)$$

for a given collapse operator \hat{x} acting on the state at rate Γ_x . In our case $\hat{x} = \{a, \sigma_i^-, \sigma_i^+\}$ (with $i = 1, \dots, N$) and $\Gamma_x = \{\kappa, \Gamma_\downarrow, \Gamma_\uparrow\}$ for the cavity losses, free-space spontaneous emission and incoherent pumping processes, respectively. The density matrix time evolution is then governed by the following master equation:

$$\partial_t \rho = -i[H_G, \rho] + \sum_{\alpha} \mathcal{L}[\hat{x}_\alpha] \rho \quad (14)$$

where the summation index runs over all the collapse operators previously defined. From Eq.(14) we can also derive the differential equation governing the dynamics of the expectation value of a time-independent observable \hat{A} (the so-called Heisenberg-Langevin equations):

$$\partial_t \langle \hat{A} \rangle = i \langle [H_G, \hat{A}] \rangle + \sum_{\alpha} \Gamma_{x_\alpha} \left[\langle \hat{x}_\alpha^\dagger \hat{A} \hat{x}_\alpha \rangle - \frac{1}{2} \langle \{ \hat{x}_\alpha^\dagger \hat{x}_\alpha, \hat{A} \} \rangle \right]. \quad (15)$$

III. RESULTS: FULL MODEL

After having revisited the two well known Dicke and Tavis-Cummings models, here we study the full model

given by Eq.(14). In order to derive the phase diagram in the thermodynamic limit, we first perform a linear stability analysis in the mean-field approximation, where we impose that the light and atomic operators are completely decorrelated. Then, we perform a full quantum calculation and numerically evaluate the observables corresponding to photon number in the cavity mode and atomic excited state population, using exact diagonalization for a small system size of $N = 8$ atoms and $N = 10$ photons. Finally, we show an example of the spectrum of the emitted light for different phases of the phase diagram.

A. Mean-field and linear stability analysis of the phase diagram

We will first obtain the phase diagram in the thermodynamic limit ($N \rightarrow \infty$) with a mean-field approximation, where we assume that the atomic and photonic operators are completely decorrelated. Using Eq.(15) and assuming the system is homogeneous, we derive the equations of motion for the expectation values $\langle a \rangle$, $\langle \sigma^- \rangle \equiv \sum_i \langle \sigma_i^- \rangle / N$ and $\langle \sigma^z \rangle \equiv \sum_i \langle \sigma_i^z \rangle / N$:

$$\begin{aligned} \partial_t \langle a \rangle &= -i\tilde{\omega}_c \langle a \rangle - i \left(\lambda \langle \sigma^- \rangle + \lambda' \langle \sigma^- \rangle^* \right) \\ \partial_t \langle \sigma^- \rangle &= -i\tilde{\omega}_0 \langle \sigma^- \rangle + 2i \langle \sigma^z \rangle \left(\lambda \langle a \rangle + \lambda' \langle a \rangle^* \right) \\ \partial_t \langle \sigma^z \rangle &= \Gamma_T (\nu/2 - \langle \sigma^z \rangle) + \\ &\quad + 2\text{Im} \left[\lambda \langle a \rangle \langle \sigma^- \rangle^* - \lambda' \langle a \rangle \langle \sigma^- \rangle \right], \end{aligned} \quad (16)$$

with $\tilde{\omega}_c \equiv \omega_c - i\kappa/2$, $\tilde{\omega}_0 \equiv \omega_0 - i\Gamma_T/2$, $\Gamma_T \equiv \Gamma_\uparrow + \Gamma_\downarrow$ and $\nu \equiv (\Gamma_\uparrow - \Gamma_\downarrow)/\Gamma_T$. These expressions have been obtained at the mean-field level, by approximating the expectation values $\langle a^\dagger \sigma^\alpha \rangle \approx \langle a^\dagger \rangle \cdot \langle \sigma^\alpha \rangle$ (with $\alpha = +, -, z$), that is, we consider that the photonic and atomic degrees of freedom are decorrelated.

In order to study the stability of the normal phase we then perform a perturbation on the normal state, that is, we assume our operators to be of the form $\hat{x} = \langle \hat{x} \rangle_{\text{NS}} + \delta \hat{x}$, with $\langle \hat{x} \rangle_{\text{NS}}$ denoting the expectation value of the operator in the normal phase and $\delta \hat{x}$ is the perturbation. In the normal phase $\langle a \rangle_{\text{NS}} = \langle \sigma^- \rangle_{\text{NS}} = 0$ and $\langle \sigma^z \rangle_{\text{NS}} = -1$. Therefore, the time evolution of the expectation value of the operators is just given by the perturbation term, that is $\partial_t \langle \hat{x} \rangle = \partial_t \langle \delta \hat{x} \rangle$. Replacing this in Eq. (16) the expression for the operators and only keeping linear perturbation terms (neglecting higher order terms), we obtain a 4x4 matrix for the time evolution of the expected value of the operators a , a^\dagger , σ^+ and σ^- :

$$\partial_t \begin{pmatrix} \langle \delta a \rangle \\ \langle \delta a^\dagger \rangle \\ \langle \delta \sigma^- \rangle \\ \langle \delta \sigma^+ \rangle \end{pmatrix} = \begin{pmatrix} -i\tilde{\omega}_c & 0 & -i\lambda & -i\lambda' \\ 0 & i\tilde{\omega}_c^* & i\lambda' & i\lambda \\ i\nu\lambda & i\nu\lambda' & -i\tilde{\omega}_0 & 0 \\ -i\nu\lambda' & -i\nu\lambda & 0 & i\tilde{\omega}_0^* \end{pmatrix} \begin{pmatrix} \langle \delta a \rangle \\ \langle \delta a^\dagger \rangle \\ \langle \delta \sigma^- \rangle \\ \langle \delta \sigma^+ \rangle \end{pmatrix}. \quad (17)$$

$\langle \sigma^z \rangle$ terms have been purposely left behind as (in linear order) they only couple to themselves and do not

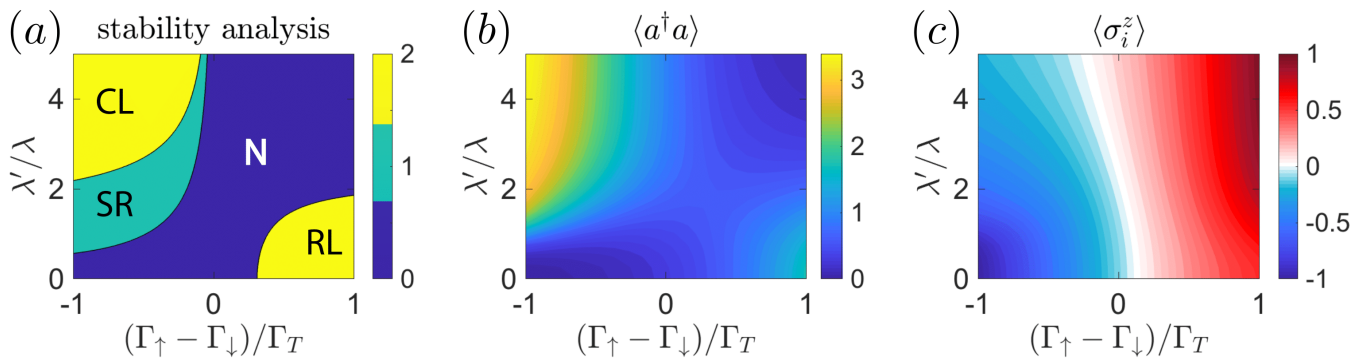


FIG. 1: Phase diagram of (a) the stability analysis, (b) the expected value of the number of photons and (c) the expected value of the spin inversion. In all graphs we represent $\frac{\lambda'}{\lambda}$ versus $\frac{\Gamma_\uparrow - \Gamma_\downarrow}{\Gamma_T}$, each with its color key to help identify the different phases. Values for the constants are $\omega_c = 1$, $\kappa = 1$, $\Gamma_T = 1$, $\lambda = 0.9$, all in ω_0 units.

contribute to the stability analysis. We will now build the phase diagram. As can easily be seen in Eq. (17), when at least one of the eigenvalues of the matrix satisfies $Re > 0$, the phase will be unstable to perturbations and the photonic mode will achieve macroscopic occupation. This phase diagram is shown in Fig. (1) (a), and the different phases correspond to: In purple, the *normal* phase N with no $Re > 0$ eigenvalues, stable under perturbations. In blue, the *superradiant* phase SR, with 1 eigenvalue with $Re > 0$, with the properties discussed in section A. In yellow, 2 differentiated *lasing* phases, the *regular lasing* RL phase, associated with large values of Γ_\uparrow and small λ' , which corresponds to the phase discussed in section B. A *counter-lasing* CL phase in the large λ and Γ_\downarrow region arises due to instability induced by counter-rotating terms, but its not quite like RL, as its emission peaks in a definite frequency too, but there is no inversion of population, as can be seen in Fig. (1) (c).

B. Exact calculation for a finite number of particles

The previous mean-field analysis only works for $N \rightarrow \infty$. For a finite small value of N we need to go one step further, and perform the exact calculation that takes into account all quantum correlations between atoms and light. In order to do this, one needs to express first the Hamiltonian and Lindblad in an appropriate basis that spans the Hilbert space of the system. An intelligent choice for the computational basis is the one resulting from the product state of each atom in a well defined internal state (ground or excited state) and the photons in a Fock state (well defined number of photons in the cavity mode). Since this basis has infinite dimension (as the number of photons is not limited), one needs to truncate the photon states to a maximum number. After doing this, the stationary state can be found from the asymptotic long-time solution after numerically integrating the master equation Eq.(14), starting with an (arbitrary) initial state where all atoms are excited. The evaluation of

an observable \hat{A} (expressed in the same computational basis) is then straightforward from $\langle \hat{A} \rangle = \text{Tr}[\rho \hat{A}]$.

Constructing the full code to perform this calculation is a complex task and we (my advisor and I) have regarded it as being out of scope of the present work. Therefore, we have adapted an open source code that exploits the permutation symmetry between atoms in the system [3] to treat our particular problem. Using this, we have studied two observables that characterize the superradiant and lasing phases: the photon number in the cavity mode $\langle a^\dagger a \rangle$ and the population inversion $\langle \sigma^z \rangle$. The results are shown in Fig.1 (b) and (c), respectively, for $N = 8$ atoms and $N_{\text{ph}} = 10$ photons. We observe that both in the superradiant and in the lasing phase the cavity mode is populated by photons, while only in the regular lasing phase there is population inversion ($\langle \sigma \rangle > 0$).

C. Spectral analysis of light emitted in the superradiant and lasing phases

The spectrum of light emitted by the atoms, characterizes each of the phases and it can be useful to distinguish between the superradiant and the lasing states. Here, we study the emission spectrum, which is defined as the Fourier transform of the two-photon correlation function [4]:

$$S(\omega) = 2\text{Re} \left[\int_0^\infty \langle a^\dagger(t)a(0) \rangle e^{i\omega t} dt \right]. \quad (18)$$

The expectation value $\langle a^\dagger(t)a(0) \rangle$ can be obtained by making use of the quantum regression theorem, that tells us that this quantity is equivalent to the expectation value of the a^\dagger operator, evaluated for the time-evolved state that was initially prepared as $a\rho_{\text{ss}}$, with ρ_{ss} the steady state of the system.

In order to observe the distinct features of the spectrum we need to have a sufficiently large number of atoms. As previously mentioned, the maximum number

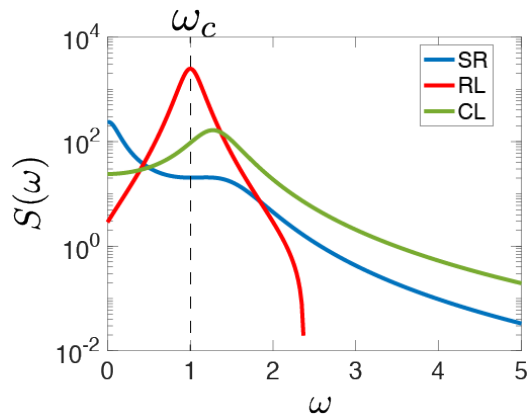


FIG. 2: Light emission spectrum for the superradiant, regular lasing, and counter lasing phases respectively. Frequency ω in ω_0 units. $S(\omega)$ axis in logarithmic scale. Values for the constants are: (SR) $\lambda' = \lambda$, $\Gamma_{\downarrow} = 1$ and $\Gamma_{\uparrow} = 0$; (RL) $\lambda' = 0$, $\Gamma_{\downarrow} = 0$ and $\Gamma_{\uparrow} = 1$; (CL) $\lambda' = 3\lambda$, $\Gamma_{\downarrow} = 1$ and $\Gamma_{\uparrow} = 0$; and for all cases $\omega_c = 1$, $\kappa = 1$, $\Gamma_T = 1$, $\lambda = 0.9$, all in ω_0 units.

of atoms that we can consider in the exact calculation is strongly limited. For this reason, we will consider here a different approach based on truncating the correlations between quantum operators to second order, called second order cumulant expansion [6]. That means, we will go one step further from the mean-field calculation and treat exactly the product between two operators (see the Appendix for more details). This will allow us to obtain the two-photon correlation function $\langle a^{\dagger}(t)a(0) \rangle$ needed for the evaluation of the spectrum.

This part of the work has been done by adapting the open source library [5] to our particular problem. Using this, we have obtained the emission spectra for different values of parameters corresponding to the different phases: superradiant, regular lasing and counter-lasing. The result is shown in Fig.2. As already anticipated, the spectra is very different in these three cases. For the superradiant phase the spectrum covers a broader range of frequencies, while for the lasing phases it is peaked at some particular frequency, indicating that the emitted light is mostly monochromatic. In the regular lasing phase this frequency corresponds to the one for the cavity mode ω_c , whereas for the counter-lasing phase it is shifted to a different value.

IV. CONCLUSIONS

We have presented the Dicke and Tavis-Cummings models and analyzed their superradiant and lasing phase transitions. We then have generalized the model and made it more realistic by adding cavity photon losses, spontaneous emission and incoherent pumping, as well as making the relative strength between co-rotating and counter-rotating coupling terms tunable. With such a model, we were able to construct a phase diagram in the $(\nu, \frac{\lambda'}{\lambda})$ space. Firstly, we used the mean-field approximation and linearized our model (neglecting second order operators) by considering complete decorrelation of the atomic and photonic operators, to check whether a phase was stable under perturbations. Next, we have gone beyond mean-field (which only works for $N \rightarrow \infty$) and considered the exact quantum calculation by integrating the master equation for a reduced number of particles, and evaluated the expectation value of the number of atoms $\langle a^{\dagger}a \rangle$ and the spin inversion $\langle \sigma_z \rangle$ and represented it in the same $(\nu, \frac{\lambda'}{\lambda})$ space. Our results are in perfect agreement with [6] and [7]. Finally, we compared the light emission spectrum of the three phases and observed clear differences between them, notably a very pronounced peak in the regular lasing phase. Further extension of this work could include the generalization to more complex types of cavities, such as multimode or ring cavities that respect the continuous translational symmetry of the system, and for which more exotic phases are expected to emerge.

Acknowledgments

I would like to thank everyone that has been around me through these atypical times, my family, my friends, my colleagues and my girlfriend, they have all contributed to me getting this work done and finishing my degree. I want to show special gratitude to Mariona, my advisor, who not only has helped me immensely throughout this work, but also reignited the spark of my passion for this subject, physics, and I will always be grateful to her for it.

[1] R. Dicke, “Coherence in Spontaneous Radiation Processes”, *Phys. Rev.* **93**: 99-110 (1954).
[2] K. Hepp, “On the superradiant phase transition for molecules in a quantized radiation field: the Dicke maser model”, *Annals of Physics*, **76**(2), 360-404 (1973).
[3] P. Kirton, ”Peterkirton/permutations: permutations v1.0” 2017, <https://doi.org/10.5281/zenodo.376621>
[4] M. O. Scully et al, “Quantum Optics”, Cambridge University Press (1997).

[5] D. Plankensteiner et al., “QuantumCumulants.jl: A Julia framework for generalized mean-field equations in open quantum systems”, arXiv:2105.01657 (2021).
[6] P. Kirton et al., “Superradiant and lasing states in driven-dissipative Dicke models”, *New J. Phys.* **20**: 015009 (2018).
[7] P. Kirton et al., “Suppressing and restoring the Dicke superradiance transition by dephasing and decay”, *Physical review letters*, **118**(12): 123602 (2017).

Appendix A: Emission spectrum using second order cumulant expansion

As mentioned in the main text, the second order cumulant expansion consists of treating in an exact way the expectation value of the product of two operators such as $\langle a^\dagger a \rangle$, $\langle a\sigma^+ \rangle$, $\langle a\sigma^- \rangle$, $\langle \sigma^+ \sigma^- \rangle$ and $\langle \sigma^+ \sigma^+ \rangle$ (and the corresponding conjugate values). By using Eq.(15), and neglecting higher order correlation terms, it is possible to obtain a complete set of differential equations describing the evolution of these expectation values in time [6]. We can then find the steady state by numerically integrating the set of differential equations, and finding the asymptotic value in the long time limit.

Once the steady state is found, we can apply the quantum regression theorem and find the time-delayed correlation functions by further evolving the expectation values according to (the steady state is taken as the initial state for the evolution) [6]:

$$\frac{d\mathbf{C}}{dt} = \mathcal{M}\mathbf{C}(t) \quad (\text{A1})$$

with

$$\mathbf{C}(t) = \begin{pmatrix} \langle a^\dagger(t)a(0) \rangle \\ \langle a(t)a(0) \rangle \\ \langle \sigma^+(t)a(0) \rangle \\ \langle \sigma^-(t)a(0) \rangle \end{pmatrix} \quad (\text{A2})$$

and

$$\mathcal{M} = \begin{pmatrix} i\tilde{\omega}_c & 0 & i\lambda & i\lambda' \\ 0 & -i\tilde{\omega}_c^* & -i\lambda' & -i\lambda \\ -i\lambda \langle \sigma^z \rangle_{\text{ss}} & -i\lambda' \langle \sigma^z \rangle_{\text{ss}} & i\tilde{\omega}_0 & 0 \\ i\lambda' \langle \sigma^z \rangle_{\text{ss}} & i\lambda \langle \sigma^z \rangle_{\text{ss}} & 0 & -i\tilde{\omega}_0^* \end{pmatrix}, \quad (\text{A3})$$

where $\langle \sigma^z \rangle_{\text{ss}}$ is the steady state expectation value.

After solving this set of differential equations to find $\langle a^\dagger(t)a(0) \rangle$ it is straightforward to evaluate the Fourier transform in Eq.(18) that defines the spectrum.